Cellular/Molecular

Ca^{2+} Regulation of Dynamin-Independent Endocytosis in Cortical Astrocytes

Min Jiang and Gong Chen
Department of Biology, Huck Institutes of Life Sciences, The Pennsylvania State University, University Park, Pennsylvania 16802

Astrocytes release ATP and glutamate through vesicular exocytosis to mediate neuron–glial interactions. In contrast to exocytosis, the endocytic pathways in astroglial cells are poorly understood. Here, we identify a constitutive endocytic pathway in cultured astrocytes that is dependent on neither clathrin nor dynamin. This dynamin-independent endocytic pathway is regulated by Rab5, an early endosome protein. The endocytosed vesicles show fast transition from early endosomes to late endosomes and lysosomes within a few minutes. Interestingly, this clathrin- and dynamin-independent endocytosis in astrocytes is potently regulated by intracellular Ca^{2+}. ATP and glutamate greatly enhance the dynamin-independent endocytosis through elevating the intracellular Ca^{2+}. In addition, amyloid-β peptide (Aβ) also enhances the dynamin-independent endocytosis by inducing Ca^{2+} transients in astrocytes. These results demonstrate a novel endocytic pathway in glial cells that is dynamin independent but tightly regulated by intracellular Ca^{2+}. The regulation by ATP, glutamate, and Aβ suggests an important role of the dynamin-independent endocytosis in both physiological and pathological conditions.

Introduction

Endocytosis is a fundamental cellular function involved in nutrient uptake, pathogen removal, and transporting signaling molecules from extracellular environment to intracellular cytoplasm. Endocytosis includes phagocytosis, which internalizes large particles, and pinocytosis, which internalizes membrane proteins, lipids, and fluid with soluble molecules (Conner and Schmid, 2003). Among pinocytosis, macropinocytosis, and clathrin- or caveolin-dependent endocytosis have been extensively studied. The clathrin-mediated endocytosis plays an important role in cell signaling through the trafficking of membrane receptors (Benmerah and Lamaze, 2007). After clathrin-mediated endocytosis, the clathrin coat will be dissociated and the uncoated vesicles will fuse with early endosomes to sort out endocytosed molecules. Some receptors will be recycled back to the plasma membrane, whereas others will be transported to Golgi for signal processing or destined to lysosomes for degradation (Maxfield and McGraw, 2004). The clathrin-independent endocytic pathways are much less understood, except caveolar endocytosis, which is mediated by caveolin-dependent membrane invaginations named caveolae (Cheng et al., 2006; Parton and Simons, 2007). Caveolae are relatively stationary membrane structures and are thought to harbor many enzymes to facilitate compartmental cell signaling (Pelkmans and Helenius, 2002; Thomsen et al., 2002). Both clathrin- and caveolin-mediated endocytosis are dependent on a GTPase dynamin, which forms a ring on the neck of invaginated pits after initial endocytosis and pinches off vesicles from the plasma membrane (Sever, 2002). In contrast, very little is known about clathrin- and caveolin-independent endocytosis, although such endocytic pathway has long been recognized in many cell types (Lamaze and Schmid, 1995; Lamaze et al., 2001; Sabharanjak et al., 2002; Kirkham et al., 2005; Mayor and Pagano, 2007; Vidricaire and Tremblay, 2007).

In mammalian brains, astrocytes play critical roles in supporting and regulating neuronal functions. Astrocytes send out endfoot protrusions to wrap around capillaries and form the blood–brain barrier with endothelial cells. Endocytosis in the endfeet of astrocytes is believed to be important for nutrient uptake from capillaries. However, the endocytic pathways in astroglial cells are mostly unexplored. In contrast, exocytosis in astrocytes has been well studied, especially with regard to the release of gliotransmitters including ATP and glutamate (Bezzi et al., 2004; Kreft et al., 2004; Zhang et al., 2004b, 2007; Chen et al., 2005; Jourdain et al., 2007).

We used a live fluorescence imaging technique to investigate endocytic pathways in cultured cortical astrocytes. We identified a constitutive endocytic pathway in astrocytes that is neither clathrin nor caveolin dependent. This endocytic pathway is also dynamin independent but is regulated by early endosomal protein Rab5. Interestingly, we found that this dynamin-independent endocytosis is tightly regulated by intracellular Ca^{2+} and greatly enhanced by ATP and glutamate. Furthermore, amyloid-β peptide (Aβ) also significantly increases the dynamin-independent endocytosis in astrocytes, suggesting that malfunction of astroglial endocytosis may contribute to neurological disorders.

Received Dec. 23, 2008; revised April 9, 2009; accepted May 16, 2009.

This work was supported by National Science Foundation Grant 0236429, National Institutes of Health Grant NS54858, and American Heart Association Grant 0765258U (G.C.). We thank Drs. Matthew Whim, Zuhang Sheng, Bernhard Luscher, and Yong-Jian Liu for careful reading of this manuscript and insightful comments. We also thank Ru-Bing Chen for her illustrative work on the summary model.

Correspondence should be addressed to Dr. Gong Chen, Department of Biology, 201 Life Sciences Building, Huck Institutes of Life Sciences, The Pennsylvania State University, University Park, PA 16802. E-mail: gongchen@psu.edu.

DOI:10.1523/JNEUROSCI.6139-08.2009

 0270-6474/09/298063-12$15.00/0

Materials and Methods

Astroglial culture. Astroglial cultures were prepared from newborn Sprague Dawley rats [postnatal day 2 (P2) to P3] similar to those described previously (McCarthy and de Vellis, 1980; Yao et al., 2006). In brief, cortex tissue was dissected out and incubated for 30 min in 0.05% trypsin-EDTA solution. After enzyme treatment, tissue blocks were triturated gently and dissociated cells were plated onto 25 cm^2 flasks and maintained for 5–7 d. During the first week after plating, flasks were shaken rigorously to remove neurons and other nonastrocytic cells until astrocytes reached confluence before being seeded onto coverslips. The culture medium contained 500 ml of MEM (Invitrogen), 5% fetal bovine serum (HyClone), 100 mg of $NaHCO_3$, 20 mM D-glucose, 2.5 mM L-glutamine, and 25 U/ml penicillin/streptomycin. Cells were maintained in 5% CO_2 incubator at 37°C for 2–3 weeks.

DNA transfection. Cells were transfected with a modified Ca^{2+}-phosphate transfection protocol developed in our laboratory (Jiang and Chen, 2006). DNA/Ca^{2+}-phosphate precipitate was prepared by using the Clontech CalPhos Mammalian Transfection kit (BD Biosciences). Cells were incubated in the presence of the precipitate for 30–60 min in 5% CO_2 culture incubator. Usually after 24–48 h of transfection, cells were taken out for experiments.

Immunostaining. For immunostaining, cells were washed three times in PBS, fixed in 4% paraformaldehyde for 12 min, and permeabilized for 5–15 min with 0.01–0.2% Triton X-100 in PBS containing 10% donkey serum. After a brief wash in PBS, cells were incubated with primary antibodies overnight at 4°C. The secondary antibodies conjugated with Alexa fluorophores were used to detect primary antibodies. Fluorescence signals were visualized with an Olympus confocal microscope (Olympus Fluoview FV 1000) or a Zeiss Axioplan 2 microscope.

Primary antibodies were as follows: rabbit anti-GFAP (1:800 dilution; Promega), mouse monoclonal anti-clathrin (1:500; Santa Cruz Biotechnology), mouse anti-caveolin-1 (1:100; BD Transduction Laboratories), mouse anti-EEA1 (1:300; BD Transduction Laboratories), and anti-LAMP1 (1:200; Assay Designs).

Secondary antibodies were as follows: Alexa Fluor 488-conjugated goat anti-rabbit (1:1000 dilution; Invitrogen) and Alexa Fluor 647-conjugated goat anti-mouse (1:1000 dilution; Invitrogen).

A fixable FM1-43 (Invitrogen) or a fixable version of FM4-64 (FM4-65; Biotium) was used in some experiments to view FM signal after immunocytochemistry.

FM imaging. Astrocytes were used after 2–20 d *in vitro* (DIV), with the majority between 7 and 14 DIV. Coverslips were transferred into a perfusion chamber mounted on a microscope stage and continuously perfused with a bath solution containing 128 mM NaCl, 30 mM D-glucose, 25 mM HEPES, 5 mM KCl, 2 mM $CaCl_2$, and 1 mM $MgCl_2$, pH 7.3, adjusted with NaOH. For most experiments, cells were stained with bath solution containing 10–20 μM FM1-43 or FM4-64 for 1.5–5 min and then washed with ADVASEP-7 for 5 min to remove the nonspecific background signal (Kay et al., 1999). Fluorescence signal of FM dye was visualized on a Nikon TE-2000-S microscope and analyzed using Simple PCI imaging software (C-Imaging). To quantify the intensity of fluorescent signals, the mean intensity of each individual astrocyte was measured with Simple PCI imaging software and then averaged across different cells. The background signal in nonastrocytic area was subtracted. For easy comparison, the fluorescent intensity of testing groups was normalized to the control group. Student's *t* test was used to test statistical significance between control and experimental groups except as stated otherwise.

Ca^{2+} imaging. Cells were incubated in bath solution (128 mM NaCl, 30 mM D-glucose, 25 mM HEPES, 5 mM KCl, 2 mM $CaCl_2$, and 1 mM $MgCl_2$, pH 7.3, adjusted with NaOH) containing 10 μM fura-2 AM (Invitrogen) for 45 min at 37°C. After dye loading, coverslips were transferred to a perfusion chamber mounted on a Nikon TE-2000-S inverted microscope with a 40× objective and a high 340/380 nm transmittance filter for Ca^{2+} ratio imaging (Chroma Technology). Cells were then washed for 15 min in bath solution with a perfusion rate of 1–2 ml/min. Images were collected from randomly selected areas in astrocytes. Calcium signals were presented as ratios of the fluorescent emission signals after excitation at 340 and 380 nm, correspondingly, and processed by Simple PCI imaging software (C-Imaging). The calibration of fura-2 AM fluorescent signals was performed by using a fura-2 calcium imaging calibration kit (Invitrogen; F-6774). Briefly, a standard curve was built based on the measurement of fluorescent intensity of each individual standard solution at two excitation wavelengths (340 and 380 nm). The actual Ca^{2+} concentration was calculated according to the K_d determined from the standard curve.

Drugs and reagents. ATP, glutamate, filipin, and dynasore were purchased from Sigma-Aldrich. 5-Methylamino-2-(2*S*,3*R*,5*R*,8*S*,9*S*)-3,5,9-trimethyl-2-(1-oxo-1-(1*H*-pyrrol-2-yl)propan-2-yl)-1,7-dioxaspiro(5.5)undecan-8-yl)methyl)benzooxazole-4-carboxylic acid (A23187), thapsigargin, 2-aminoethoxydiphenyl borate (2-APB), and α-methyl-4-carboxyphenylglycine (MCPG) were bought from Tocris. Aβ25–35, Aβ1–42, and their reverse peptides were purchased from American Peptide Company. Fluor 555 Aβ1–42 was purchased from AnaSpec. FM1-43, fixable FM1-43, Lysotracker, FM4-64, 2′(3′)-*N*-methylanthraniloyl-ATP (MANT-ATP), and Alexa Fluor 647-conjugated transferrin were purchased from Invitrogen. BODIPY FL C5-lactosylceramide complexed to BSA was purchased from Invitrogen. The enhanced green fluorescent protein (EGFP)-tagged wild-type (WT) and dominant-negative (DN) (K44A) dynamin plasmids were gifts from Dr. Pietro De Camilli (Yale University School of Medicine, New Haven, CT). The EGFP-tagged Rab5 WT, Rab5S34N, and Rab5Q79L plasmids were obtained from Dr. Yong-jian Liu (University of Pittsburgh, Pittsburgh, PA). The Golgi marker EGFP-GalT was from Dr. Brian Storrie (University of Arkansas for Medical Sciences, Little Rock, AR). The EGFP-clathrin heavy chain short hairpin RNA (shRNA) was a gift from Dr. Liangyi Chen (Institute of Biophysics, Chinese Academy of Science, Beijing, China). The wild-type and dominant-negative EGFP-tagged caveolin-1 constructs were offered by Dr. Coyne Carolyn (University of Pittsburgh School of Medicine, Pittsburgh, PA).

Results

Basal constitutive endocytosis in astrocytes

To study astroglial endocytosis, we used live fluorescence imaging and cortical astrocyte cultures, in which the majority of cells (>95%) are immunopositive for glial fibrillary acidic protein (Fig. 1*A*). Small fluorescent dye FM1-43 has been widely used in studying synaptic vesicle endocytosis and exocytosis at nerve terminals (Betz and Bewick, 1992). FM imaging has also been used to monitor vesicle trafficking in astrocytes (Krzan et al., 2003; Chen et al., 2005; Zhang et al., 2007). We found that a brief exposure to FM1-43 (20 μM; 3 min) in normal bath solution resulted in punctate staining (Fig. 1*B*,*C*). The nonspecific binding of FM dye on membrane surface had been washed off in the presence of ADVASEP-7 (Kay et al., 1999). The average number of FM puncta in each astrocyte is 610 ± 43 (n = 24). The uptake of FM dye by astrocytes in the absence of any stimulation is likely a constitutive form of endocytosis. To test this idea, astrocytes were repetitively stained with FM1-43 in bath solution. The accumulative FM signal significantly increased after each round of staining (4 min/round) (Fig. 1*D–F*). Quantitative analysis showed that the FM fluorescence intensity displayed a staircase increase after repeated staining, suggesting a constitutive endocytosis in astrocytes (Fig. 1*G*). To investigate the kinetics of the FM dye uptake in astrocytes, we have examined the FM signal with both brief exposure (within 2 min) and long-term exposure (up to 1 h) (supplemental Fig. 1, available at www.jneurosci.org as supplemental material). Within 2 min exposure to FM1-43, the FM staining is linearly increased with exposure time (supplemental Fig. 1*A*, available at www.jneurosci.org as supplemental material). For long-term exposure, the slope of the FM intensity curve decreased after 15 min exposure but still did not reach plateau after 1 h exposure, further suggesting a nature of constitutive endocytosis (supplemental Fig. 1*B*, available at www.jneurosci.org as supplemental material). Interestingly, the FM dye-labeled vesicles in astrocytes were highly mobile (supple-

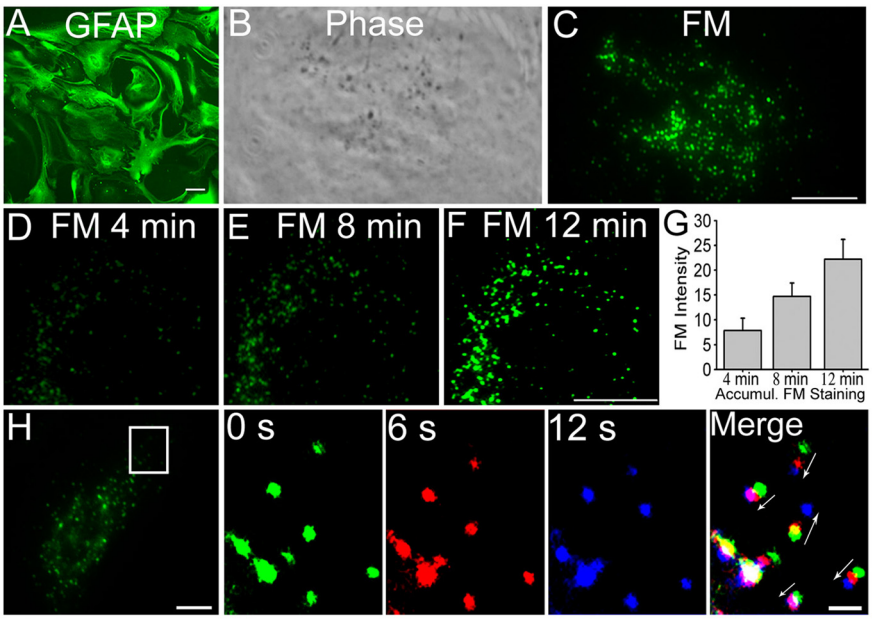

Figure 1. Live imaging of constitutive endocytosis in cortical astrocytes. ***A***, A typical immunofluorescence image of cultured glial cells stained with anti-GFAP antibody. Almost all cells were GFAP positive. ***B***, ***C***, Representative images showing phase image (***B***) and FM1-43-labeled fluorescent puncta (***C***) in a cultured astrocyte. Astrocytes were incubated with FM1-43 (20 μM) in bath solution for 5 min. ***D–F***, Accumulative FM signal after constitutive endocytosis in astrocytes. Astrocytes were exposed to FM1-43 for three consecutive rounds (4 min/round) for live staining, with a 10 min washing interval between each round. ***G***, Quantitative changes of the average FM intensity of astrocytes after multiple rounds of FM staining ($n = 6$; $p < 0.001$, one-way ANOVA test). Error bars indicate SEM. ***H***, Time-lapse images illustrating dynamic movement of FM dye-labeled vesicles. FM dye-labeled puncta were accumulating in the perinuclear area. The color-coded images illustrate the position of FM dye-labeled vesicles at different time points. The merged image showed a clear movement of vesicles toward the perinuclear area with one vesicle moving at opposite direction (arrows point to moving direction, from green to blue position). Scale bars: ***A***, 50 μm; ***B–H***, 20 μm; enlarged images of ***H***, 2 μm.

mental Movie 1, available at www.jneurosci.org as supplemental material). Time-lapse imaging revealed that the majority of FM dye-labeled vesicles moved rapidly in the cytoplasm and gradually accumulated in the perinuclear area (Fig. 1*H*). The rapid movement of FM dye-labeled vesicles is dependent on microtubules, since depolymerizing microtubules with colchicine or nocodazole essentially abolished the vesicle movement (supplemental Movie 2, available at www.jneurosci.org as supplemental material). Thus, live fluorescence imaging with FM dye revealed a constitutive endocytosis in cultured astrocytes.

The constitutive endocytosis in astrocytes is clathrin independent

Clathrin-mediated endocytosis is a major form of endocytosis involved in the recycling of cell surface receptors (Mousavi et al., 2004). To determine whether the FM dye-labeled endocytosis in astrocytes is clathrin mediated, we first compared it with a typical clathrin-mediated endocytic pathway labeled by transferrin. Previous studies have shown that cultured rat cortical astrocytes do express transferrin receptors (Qian et al., 1999). To investigate whether FM dye-labeled constitutive endocytosis is clathrin dependent, we performed live FM1-43 imaging (Fig. 2*A*) followed by immediate fixation and immunostaining with antibodies against clathrin light chain (Fig. 2*B*). As shown in the merged picture of Figure 2*C*, the FM and clathrin signals showed distinct staining patterns. In the next set of experiments, we expressed EGFP-tagged clathrin light chain in astrocytes (Fig. 2*D*). Cells were then stained with a red-shifted fixable dye FM4-65 (Fig. 2*E*) and fixed immediately to stop any vesicle movement. The merged image showed that the FM puncta (Fig. 2*F*, red) are clearly separated from the clathrin puncta (Fig. 2*F*, green). Moreover, we used clathrin heavy chain (chc) shRNA to knockdown clathrin level in astrocytes (He et al., 2008). Control experiments showed that chc shRNA significantly inhibited the endocytosis of transferrin (Fig. 2*G–I*). In contrast, chc shRNA had little effect on FM dye uptake (Fig. 2*J–L*). Quantitative analyses were shown in Figure 2, *M* and *N*. Time-lapse imaging also revealed a much slower movement of transferrin-labeled vesicles than that of FM dye-labeled vesicles (compare supplemental Movies 1 and 3, available at www.jneurosci.org as supplemental material). Therefore, our data revealed a clathrin-independent constitutive endocytic pathway in astrocytes.

Astroglial constitutive endocytosis is caveolin independent

In astrocytes, clathrin-independent caveolar endocytosis has been reported previously (Cameron et al., 2002). To investigate whether the constitutive endocytosis in astrocytes is caveolin dependent, we performed live FM staining of astrocytes followed by retrospective immunostaining with caveolin-1, which specifically labels caveolar structures (Fig. 3*A*,*B*). From the merged image (Fig. 3*C*), we found that the majority of FM puncta (green) were distinctly separated from the caveolin-1 puncta (red). We also expressed EGFP-tagged WT caveolin-1 in astrocytes and then stained with FM4-64 to analyze the localization (Fig. 3*D*,*E*). The merged picture showed nonoverlapping distribution of the caveolin (green) and FM signal (red) (Fig. 3*F*). Next, we expressed DN caveolin-1 to examine whether FM dye uptake is inhibited (Fig. 3*G*,*H*). Quantitative analysis showed no significant difference in astrocytes expressing either WT or DN caveolin-1 (Fig. 3*I*). These results suggest that the constitutive endocytosis labeled by FM dye in astrocytes is neither clathrin nor caveolin dependent.

Astroglial constitutive endocytosis is independent of dynamin

Both clathrin- and caveolin-dependent endocytosis require dynamin, a member of superfamily of GTPases, to pinch off the invaginated membrane pits (Herskovits et al., 1993; Damke et al., 1994). A dominant-negative mutant form of dynamin (K44A) has been shown to significantly inhibit clathrin- and caveolin-mediated endocytosis (Damke et al., 1994; Dessy et al., 2000). In the meanwhile, dynamin-independent endocytosis has also been reported (Zhang et al., 2004a; Bonazzi et al., 2005; Ferguson et al., 2007; Xu et al., 2008). We sought to clarify whether the constitutive endocytosis in astrocytes is dynamin dependent or not. For control experiments, when WT and dynamin K44A were overexpressed in astrocytes, the uptake of transferrin was significantly inhibited by dynamin K44A as expected (supplemental Fig. 2*A–D*; quantified in *E*; available at www.jneurosci.org as supplemental material). In contrast, the uptake of FM dye was not blocked by mutant dynamin K44A, comparing with the WT dy-

namin (Fig. 4*A–D*; quantified in *E*). To further confirm the dynamin independence, we used dynamin-specific inhibitor dynasore to investigate the effect of dynamin on constitutive endocytosis (Macia et al., 2006; Newton et al., 2006). The uptake of FM1-43 in astrocytes was not blocked by dynasore treatment (Fig. 4*F–H*). For control experiments, the same dynasore treatment significantly inhibited transferrin endocytosis (Fig. 4*I*). Thus, the constitutive endocytosis in astrocytes is a dynamin-independent endocytic pathway.

Rab5 regulates dynamin-independent endocytosis in astrocytes

In mammalian cells, endocytosed vesicles are often sorted first into early endosomes before further delivered into other organelles such as late endosomes or Golgi complex (Gruenberg, 2001; Sorkin and Von Zastrow, 2002). Since the FM dye-labeled dynamin-independent endocytosis is independent of clathrin and dynamin, it raises the question whether FM dye-labeled vesicles are sorted through early endosomes or not. To answer this question, we investigated whether the dynamin-independent endocytosis in astrocytes was affected by a small GTPase Rab5, which functions specifically in the formation and trafficking of early endosomes. Cells were transfected with either wild-type GFP-Rab5, or a constitutively active mutant Rab5 (Q97L), or a dominant-negative mutant Rab5 (S34N) (Stenmark et al., 1994). After 48 h of transfection, WT Rab5 showed no obvious effect on the FM dye-labeled dynamin-independent endocytosis (Fig. 5*A*,*B*). In contrast, the dominant-negative Rab5S34N significantly inhibited the uptake of FM dye compared with the nontransfected astrocytes (asterisk) (Fig. 5*C*,*D*; quantified in *E*) ($n = 13$; $p < 0.001$ in comparison with control). Supplemental Figure 3 (available at www.jneurosci.org as supplemental material) shows that Rab5S34N also essentially abolished the endocytosis of transferrin as expected. However, overexpression of constitutively active Rab5Q79L resulted in the appearance of enlarged early endosomes (Fig. 5*F*, arrows), possibly because of enhanced homotypic endosomal fusion as previously reported (Roberts et al., 1999; Rink et al., 2005). Interestingly, in Rab5Q79L-transfected cells, FM dye often accumulated in the enlarged early endosomes (Fig. 5*G*,*H*). To confirm that the Rab5Q79L-enlarged vesicles are indeed early endosomes, we performed immunostaining with another early endosome marker EEA1 and found high colocalization between Rab5Q79L (green) and EEA1 (red) puncta (Fig. 5*I–K*). Furthermore, live staining with fixable FM1-43 followed by immediate fixation and retrospective immunostaining with EAA1 antibody showed a nice colocalization between FM (green) and EEA1 (red) puncta in astrocytes (Fig. 5*L–N*). These results indicate that the FM dye-labeled vesicles are first sorted through early endosomes and regulated by Rab5 proteins.

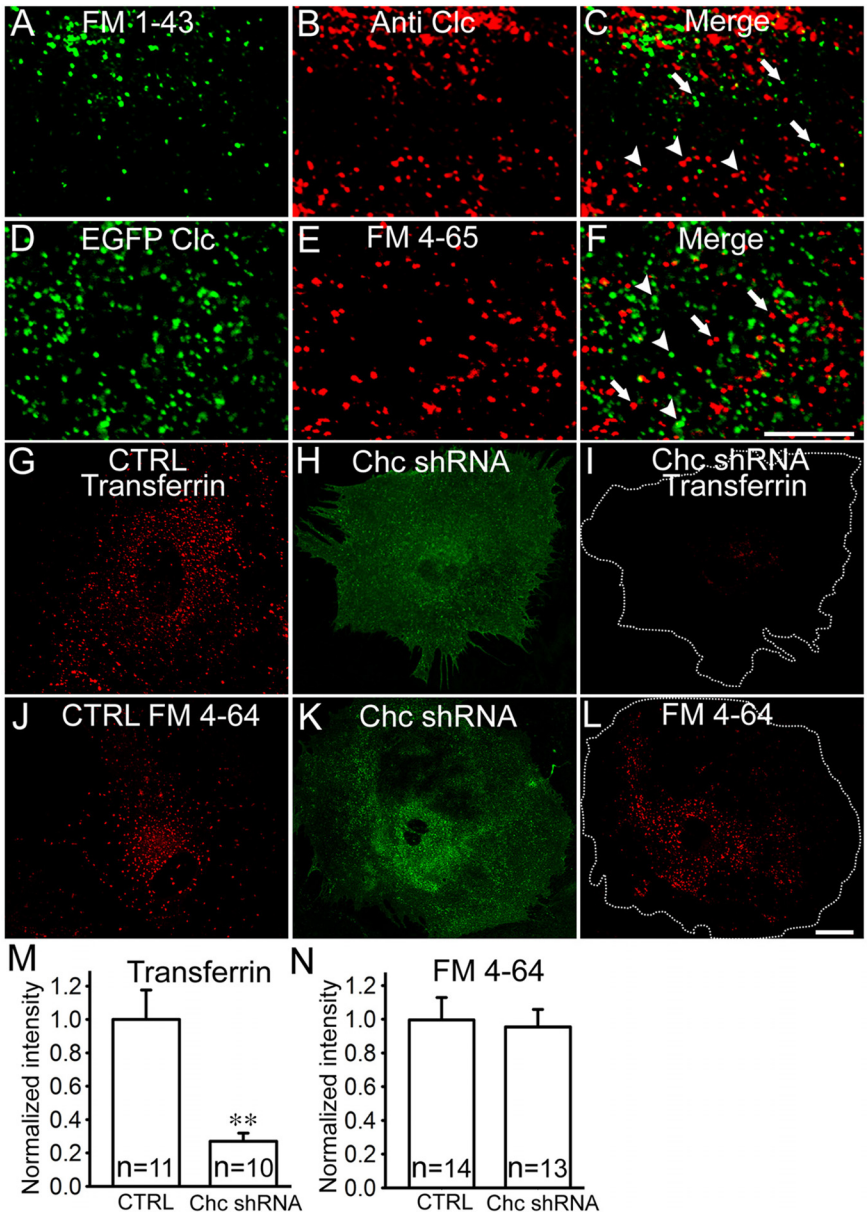

Figure 2. Constitutive endocytosis in astrocytes is not clathrin mediated. ***A***, ***B***, Fluorescent images showing the same astrocytes first stained with fixable FM1-43 in live cells (***A***) and then immunostained with anti-clathrin light chain (Clc) antibody (***B***). Cells were briefly stained with fixable FM1-43 and then fixed immediately to arrest any vesicle movement. Images were taken simultaneously after immunostaining. ***C***, Merged image showing both FM and clathrin signals. The FM puncta (green, arrows) are mostly separated from the clathrin puncta (red, arrowheads). ***D***, ***E***, Fluorescent images showing the same cells overexpressing EGFP-Clc (***D***) stained with FM4-65 (***E***) and fixed immediately after FM staining. ***F***, Merged image showing both FM and EGFP-Clc signals. The clathrin puncta (green, arrowheads) and the FM puncta (red, arrows) are mostly separated from each other. ***G***, Fluorescence image of a control astrocyte stained with Alexa Fluor 647-conjugated transferrin. ***H***, ***I***, Fluorescence images of an astrocyte overexpressing EGFP-tagged clathrin heavy chain (Chc) shRNA (***H***) and then live stained with transferrin (***I***). The transferrin signal was significantly reduced after knockdown clathrin with Chc shRNA. ***J***, Fluorescence image of a control astrocyte stained with FM4-64 (20 μM; 3 min). ***K***, ***L***, Fluorescence images of an astrocyte overexpressing Chc shRNA (***K***) and then stained with FM4-64 (***L***). The FM staining appeared not to be affected by Chc shRNA. The dotted lines in ***I*** and ***L*** delineate transfected astrocytes. ***M***, ***N***, Quantitative analysis showing that Chc shRNA induced a significant reduction in the endocytosis of transferrin ($27 \pm 5\%$ of control; $n = 10$; $^{**}p < 0.002$) but not FM dye ($96 \pm 9\%$ of control; $n = 13$; $p > 0.7$). Error bars indicate SEM. Scale bars, 20 μm.

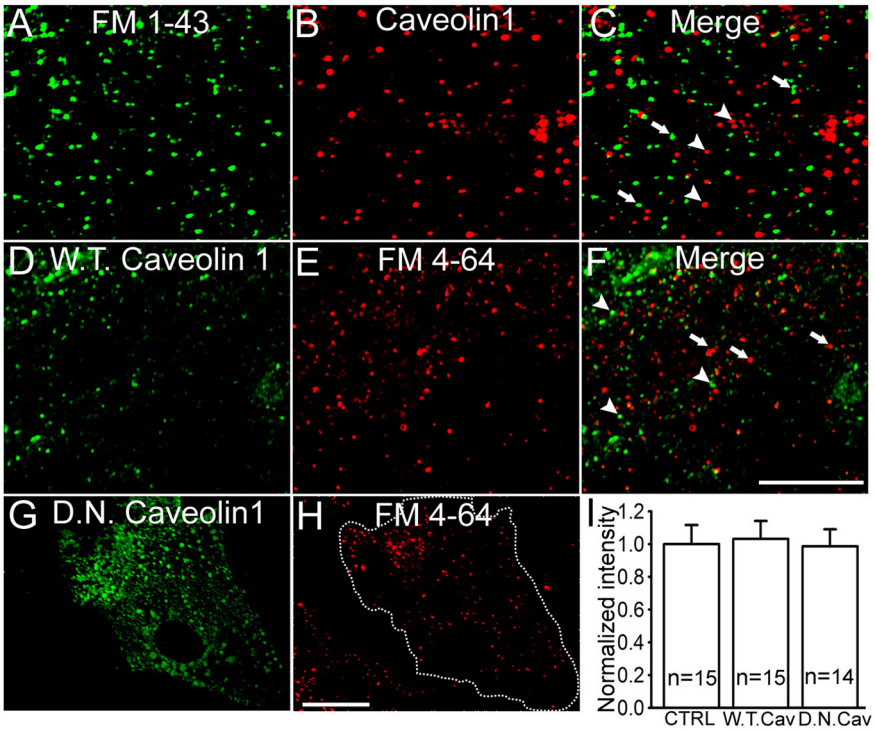

Figure 3. Constitutive endocytosis in astrocytes is caveolin independent. ***A***, ***B***, Fluorescence images showing the same astrocyte labeled by FM1-43 (***A***) followed by immediate fixation and immunostaining with anti-caveolin-1 antibody (***B***). ***C***, Merged image showing that the FM puncta (green, arrows) are distinctly separated from the caveolin-1 puncta (red, arrowheads). ***D***, ***E***, Fluorescence images showing an astrocyte overexpressing GFP-caveolin-1 (***D***) and stained with FM4-64 (***E***). After FM staining, cells were immediately fixed to arrest any vesicle movement. ***F***, Merged image showing both FM4-64 and GFP-caveolin-1 signals. The caveolin puncta (green, arrowheads) and FM puncta (red, arrows) are nonoverlapping in most cases. ***G***, ***H***, Fluorescence images of a cell overexpressing GFP-tagged dominant-negative caveolin-1 (***G***) and stained with FM4-64 (***H***). ***I***, Quantitative data showing that the FM4-64 intensity was not affected by either WT or DN caveolin-1 compared with the nontransfected control cells (WT caveolin-1, 103 ± 11% of control, $n = 15$, $p > 0.8$; DN caveolin-1, 99 ± 10% of control, $n = 14$, $p > 0.9$). Error bars indicate SEM. Scale bars, 20 μm.

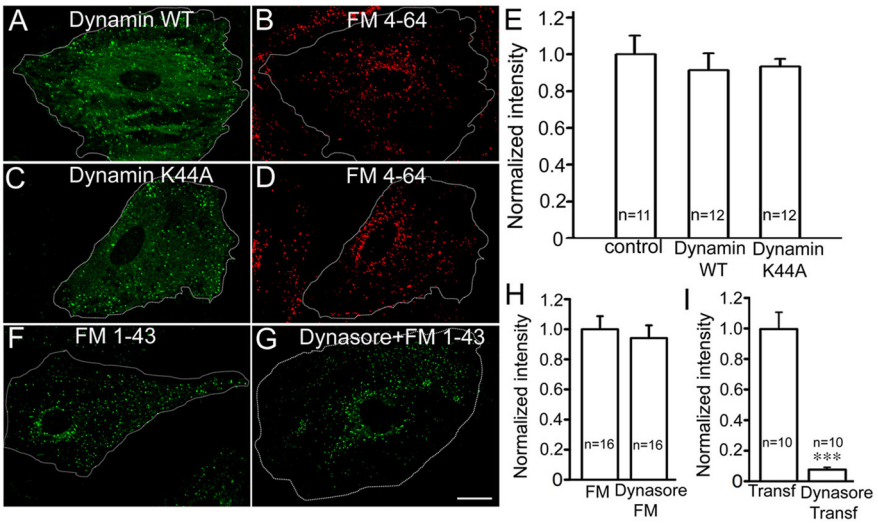

Figure 4. Constitutive endocytosis in astrocytes does not require dynamin. ***A***, ***B***, Fluorescence images of an astrocyte overexpressing GFP-WT dynamin (***A***) and stained with FM4-64 (***B***). ***C***, ***D***, Fluorescence images of an astrocyte overexpressing GFP-dynamin K44A (***C***) and stained with FM4-64 (***D***). The dotted lines delineate transfected astrocytes. ***E***, Quantitative analysis showing that neither WT nor K44A dynamin had significant effect on the uptake of FM4-64 compared with the nontransfected controls (dynamin WT, 89 ± 9% of control, $n = 12$, $p > 0.4$; dynamin K44A, 91 ± 5% of control, $n = 12$, $p > 0.5$). ***F***, ***G***, FM images of astrocytes in control (***F***) or pretreated with dynasore (50 μM; 30 min), a specific inhibitor for dynamin (***G***). ***H***, Quantitative data showing the similar FM intensity between control and dynasore-treated groups (dynasore, 94 ± 08% of control, $n = 16$, $p > 0.6$). ***I***, Quantitative data showing that the endocytosis of transferrin was significantly inhibited after dynasore treatment (dynasore, 8 ± 1% of control; $n = 10$; ***$p < 0.0001$). Error bars indicate SEM. Scale bar, 20 μm.

Rapid transition from early endosomes to late endosomes/lysosomes

After internalization, the endocytosed molecules may be destined to different intracellular organelles for signal processing or degradation (Gruenberg, 2001; Maxfield and McGraw, 2004). To test whether FM dye accumulates in the Golgi complex, we expressed a Golgi-specific marker β-1,4-galactosyltransferase (GalT) in astrocytes to illuminate Golgi in live cells. After staining with FM4-64 and allowing ~30 min for the FM dye to accumulate in the perinuclear area, we found that the majority of FM signal was adjacent to but mostly outside the Golgi complex (supplemental Fig. 4, available at www.jneurosci.org as supplemental material). Next, we investigated whether FM dye was transported to lysosomes and, if so, how fast they will appear in lysosomes. For this purpose, astrocytes were stained with fixable FM1-43 and then washed for 2, 6, or 15 min before being fixed for immunostaining with LAMP1, a specific marker for late endosomes/lysosomes (Fig. 6). For cells fixed after a 2 min washing, FM and LAMP1 signals were clearly separated (Fig. 6*A–C*), indicating that FM dye was still in early endosomes after immediate endocytosis. After 6 min of washing before fixation, some FM dye-labeled puncta were found colocalizing with LAMP1 puncta (Fig. 6*D–F*), suggesting that FM dye-labeled vesicles can fuse with or mature into late endosomes/lysosomes within a few minutes after endocytosis. With 15 min washing before fixation, the majority of FM signal was found accumulated in late endosomes/lysosomes (Fig. 6*G–I*). Thus, after internalization, FM dye can be quickly transported from early endosomes to late endosomes/lysosomes, suggesting a rapid degradation or storage system in astroglial cells.

Interestingly, in astrocytes transfected with Rab5Q79L, which enlarged early endosomes, the transportation of FM dye from early endosomes to lysosomes was significantly impaired (Fig. 6*J–M*). After Rab5Q79L transfection, we incubated astrocytes with FM4-65 for 5 min and washed for >15 min before fixation and immunostaining with LAMP1 antibody. The Rab5Q79L-enlarged early endosomes (Fig. 6*J*) never colocalized with LAMP1-labeled late endosomes/lysosomes (Fig. 6*K*), as shown by a lack of yellow signal in the merged image (Fig. 6*M*). Unexpectedly, even after extended washing after FM staining, some FM dye still accumulated inside the enlarged early endosomes (Fig. 6*M*, bottom inset), whereas other FM dye

colocalized with LAMP1-labeled late endosomes/lysosomes (Fig. 6*M*, top inset). Such a delay in the exit of FM dye from enlarged early endosomes suggests that the transition from early endosomes to late endosomes/lysosomes requires the GTP hydrolysis of Rab5 proteins (Zerial and McBride, 2001).

Dynamin-independent endocytosis of MANT-ATP and Aβ

To investigate the function of FM dye-labeled dynamin-independent endocytosis in astroglial cells, we examined what cargo other than FM dye can be internalized through this endocytic pathway. We first incubated astrocytes with FM1-43 and MANT-ATP, a fluorescent ATP analog, for 5 min in normal bath solution. After staining, live fluorescent images showed an extensive colocalization between FM dye and MANT-ATP signals (supplemental Fig. 5*A–C*, available at www.jneurosci.org as supplemental material). Like FM dye, MANT-ATP was also quickly deposited to late endosomes/lysosomes as demonstrated by colocalization with LysoTracker (supplemental Fig. 5*D–F*, available at www.jneurosci.org as supplemental material). Furthermore, the expression of dominant-negative dynamin K44A had no effect on the uptake of MANT-ATP in astrocytes (supplemental Fig. 5*G*,*H*, available at www.jneurosci.org as supplemental material), suggesting that the ATP analog is endocytosed through a dynamin-independent pathway. We also incubated astrocytes with fluorescent Aβ1–42 peptide (5 μM in bath solution) for 5 min and found punctate staining similar to FM staining pattern (supplemental Fig. 5*I*, available at www.jneurosci.org as supplemental material). The dynamin inhibitor dynasore did not block the constitutive endocytosis of Aβ1–42 (supplemental Fig. 5*J*, available at www.jneurosci.org as supplemental material). Thus, the FM dye-labeled dynamin-independent endocytosis may play an important role in the uptake or removal of molecules including ATP and Aβ peptides.

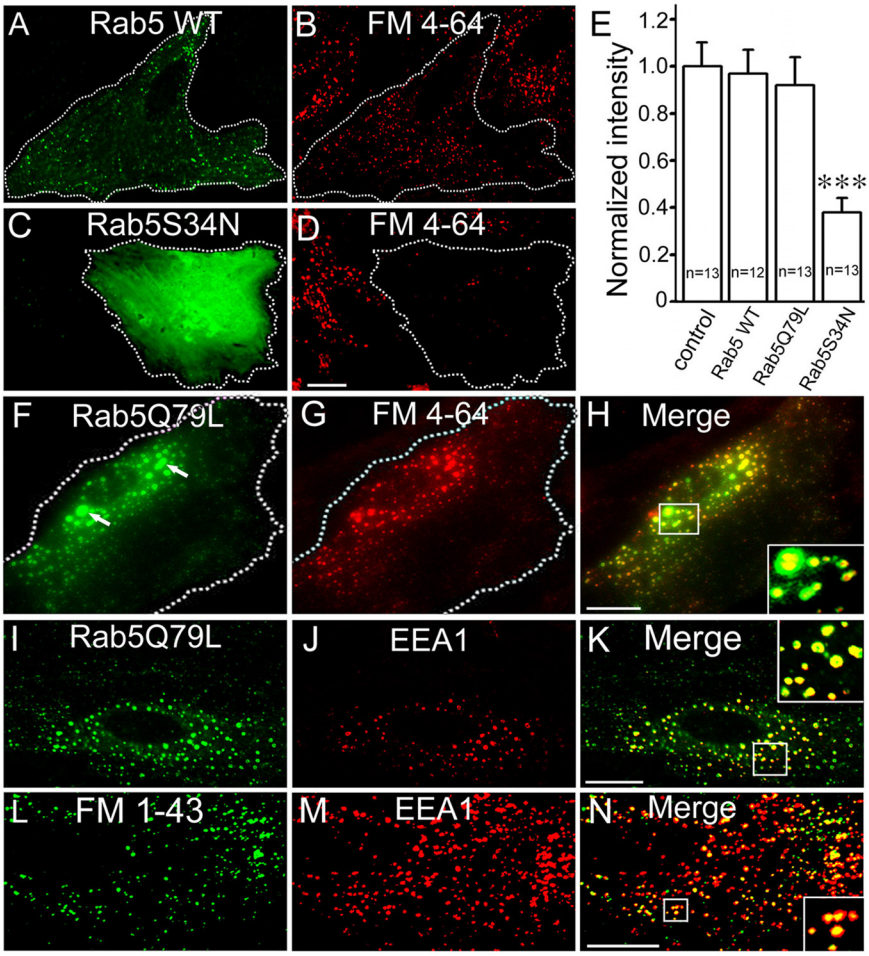

Figure 5. Dynamin-independent endocytosis in astrocytes is regulated by Rab5. ***A***, ***B***, Live fluorescence images showing that astrocytes expressing GFP-Rab5 WT (***A***) had normal uptake of FM4-64 (***B***). ***C***, ***D***, In contrast, astrocytes transfected with a dominant-negative mutant GFP-Rab5S34N (***C***) showed a significant decrease of FM dye uptake (***D***) compared with the nontransfected neighboring cells (asterisk). ***E***, Quantitative data showing the FM intensity under different Rab5-transfected groups compared with the nontransfected controls (WT Rab5, 97 ± 10% of control, $n = 12$, $p > 0.8$; Rab5Q79L, 92 ± 12% of control, $n = 13$, $p > 0.7$; Rab5S34N, 38 ± 6% of control, $n = 13$, ***$p < 0.0001$). Error bars indicate SEM. ***F***, ***G***, GFP image (***F***) and FM4-64 staining (***G***) of an astrocyte overexpressing a constitutively active form of Rab5 (GFP-Rab5Q79L). Note the large green puncta after overexpressing GFP-Rab5Q79L (***F***, arrows). ***H***, Merged image showing that the FM puncta (red) are well colocalized with Rab5Q79L-enlarged vesicles (green). The inset in the bottom corner showing an enlarged view of the boxed area. ***I–K***, Fluorescence images of an astrocyte overexpressing GFP-Rab5Q79L (***I***) and immunolabeled with the early endosome marker EEA1 (***J***). ***K***, Merged image showing that Rab5Q79L-enlarged vesicles are well colocalized with EEA1 puncta. ***L–N***, Fluorescence images of astrocytes labeled with fixable FM1-43 (***L***) and EEA1 antibodies (***M***). Cells were fixed immediately after FM staining. ***N***, Merged image showing nice colocalization between FM1-43 and EEA1 puncta, indicating that FM dye was endocytosed into early endosomes. Scale bars, 20 μm.

Astroglial dynamin-independent endocytosis is regulated by intracellular Ca^{2+}

Since the dynamin-independent endocytosis in astrocytes may function in internalizing signaling molecules, we wondered whether such endocytic pathway may be regulated by extracellular or intracellular signaling. The Ca^{2+} oscillation in astrocytes is closely associated with astroglial functions (Fiacco and McCarthy, 2006). Therefore, we first examined whether the dynamin-independent endocytosis in astrocytes is dependent on extracellular or intracellular Ca^{2+} signaling. Astrocytes were incubated with FM1-43 for 3 min in control (2 mM Ca^{2+}) or Ca^{2+}-free bath solution (Fig. 7*A*, *B*). We observed no significant difference in the uptake of FM dye by astrocytes with or without extracellular Ca^{2+} (quantified in Fig. 7*E*). We then examined whether intracellular Ca^{2+} might have any effect on the dynamin-independent endocytosis in astrocytes. A Ca^{2+} ionophore, A23187, which forms Ca^{2+} channels on the plasma membrane to allow Ca^{2+} influx, was used to increase the intracellular Ca^{2+} concentration in normal bath solution (2 mM Ca^{2+}). Remarkably, the FM dye-labeled dynamin-independent endocytosis in astrocytes was greatly enhanced with the treatment of A23187 (Fig. 7*C*,*E*) ($n = 13$; $p < 0.001$). In contrast, decreasing intracellular Ca^{2+} by pretreatment with Ca^{2+} chelator BAPTA-AM (25 μM; 45 min) significantly decreased the FM uptake by astrocytes (Fig. 7*D*,*E*) ($n = 14$; $p < 0.02$). Therefore, the FM dye-labeled dynamin-independent endocytosis in astrocytes is tightly regulated by intracellular but not extracellular Ca^{2+} signaling.

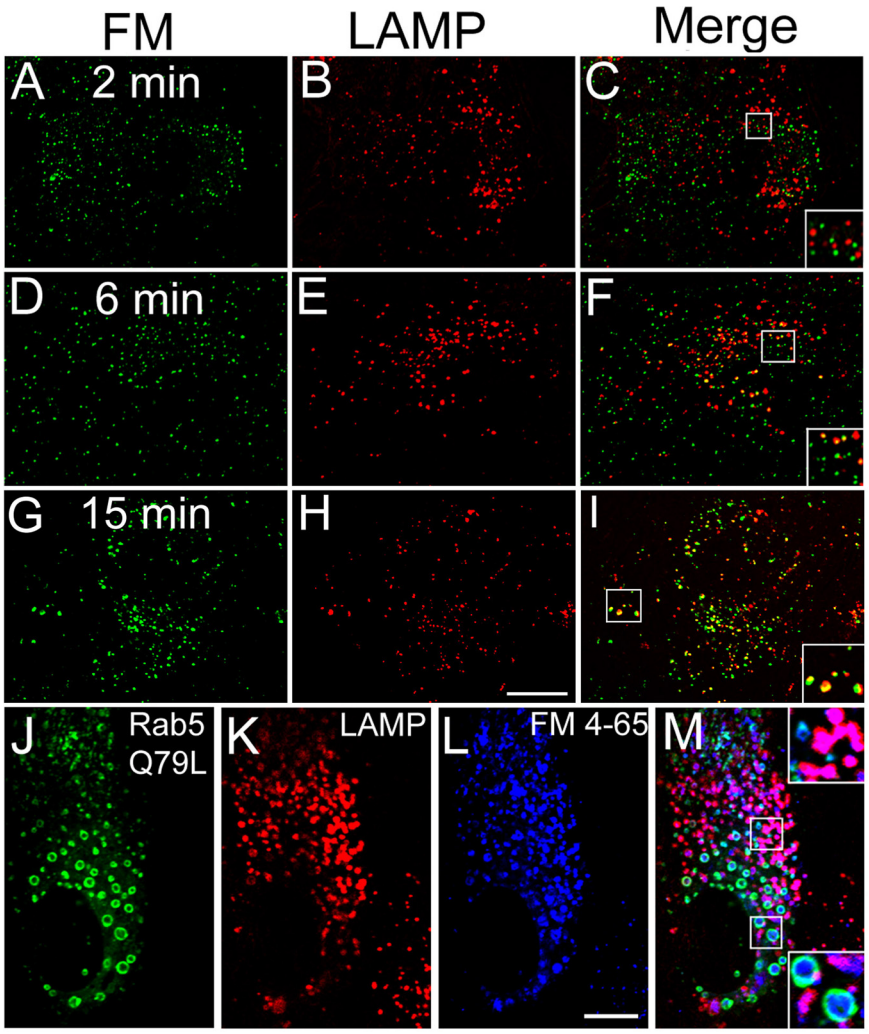

Figure 6. FM dye quickly accumulates in late endosomes/lysosomes. ***A–C***, Fluorescent images of astrocytes live stained with fixable FM1-43 (***A***), and then quickly fixed for immunostaining with LAMP1, a marker for late endosomes/lysosomes (***B***). The 2 min indicates the time interval between FM staining and fixation. The merged image (***C***) shows that, after immediate endocytosis, the majority of FM puncta (green) are not yet in late endosomes/lysosomes (red). ***D–F***, When the time interval was increased to 6 min between FM staining (***D***) and fixation for LAMP1 immunostaining (***E***), some FM puncta showed colocalization with LAMP1 (***F***; yellow puncta). ***G–I***, After a 15 min interval between FM staining and fixation, the majority of FM puncta (***G***) were well colocalized with LAMP1 (***H***), as evident from the merged image (***I***). FM and LAMP1 images were taken simultaneously after immunostaining. ***J–M***, Fluorescent images showing the colocalization of FM dye-labeled puncta with both early endosomes and late endosomes/lysosomes. ***J***, Enlarged early endosomes after the overexpression of GFP-Rab5Q79L. ***K***, Late endosomes/lysosomes labeled by LAMP1. ***L***, Fixable FM4-65 staining. ***M***, Merged images of FM4-65 (blue), GFP-Rab5Q79L (green), and LAMP1 (red). The insets are enlarged images from boxed regions. Note that some FM dyes were accumulated inside the Rab5Q79L-enlarged early endosomes (bottom inset), whereas others were colocalizing with LAMP1-labeled vesicles (top corner). Scale bars: ***A–I***, 20 μm; ***J–M***, 10 μm.

ATP regulation of the dynamin-independent endocytosis in astrocytes

ATP has been demonstrated to regulate intracellular Ca^{2+} concentration in astrocytes (Guthrie et al., 1999; Volterra and Meldolesi, 2005; Suadicani et al., 2006). We confirmed that acute application of ATP induced a significant increase of intracellular Ca^{2+} in cultured astrocytes (Fig. 8*G*). Using fura-2 calcium imaging calibration kit (Invitrogen), we estimated that the resting intracellular Ca^{2+} of astrocytes is 75 ± 5 nM ($n = 24$), and 348 ± 30 nM ($n = 24$) after ATP stimulation, similar to a previous report by Salter and Hicks (1994). Will ATP-induced Ca^{2+} increase affect the dynamin-independent endocytosis in astrocytes? To answer this question, we incubated astrocytes with FM1-43 in the presence or absence of ATP (10 μM; 90 s). ATP treatment greatly enhanced the endocytosis of FM dye compared with the control (Fig. 8*A*,*B*) ($n = 15$; $p < 0.001$). To confirm that the ATP effect is mediated by an increase of intracellular Ca^{2+}, we depleted intracellular Ca^{2+} store with pretreatment of thapsigargin, a specific intracellular Ca^{2+} pump inhibitor. Ca^{2+} imaging experiments verified that thapsigargin pretreatment (10 μM; 10 min) prevented subsequent increase of intracellular Ca^{2+} induced by ATP in astrocytes (Fig. 8*H*). Accordingly, pretreatment of astrocytes with thapsigargin essentially abolished the ATP enhancement of the FM dye uptake (Fig. 8*C*,*F*). In addition, we also used 2-APB to block IP3 receptors and found that the ATP enhancement was abolished by 2-APB (Fig. 8*D*,*F*). However, after blocking dynamin pathway with dynasore, ATP still enhanced the dynamin-independent endocytosis (Fig. 8*E*,*F*). Together, these results indicate that the dynamin-independent endocytosis in astrocytes is actively regulated by ATP through intracellular Ca^{2+} signaling.

Glutamate regulation of astroglial rapid endocytosis

Like neurons, astrocytes also release glutamate through vesicular exocytosis to affect neuron–glial interactions (Araque et al., 2000; Schools and Kimelberg, 2001; Zhang et al., 2004b). Application of glutamate onto astrocytes has been shown to trigger oscillations of intracellular Ca^{2+} via metabotropic glutamate receptors (mGluRs) (Chen et al., 1997; Fellin et al., 2006). We have confirmed in our cultured astrocytes that application of glutamate (1 mM; 5 min) evoked a significant intracellular Ca^{2+} oscillation (Fig. 9*E*). The calibrated intracellular Ca^{2+} concentration increased from a resting level of 68 ± 4 nM ($n = 22$) to 308 ± 18 nM ($n = 22$) during glutamate stimulation, consistent with a previous study by Parpura et al. (1994). The glutamate effect was mostly blocked by mGluR antagonist MCPG (Fig. 9*F*). We next examined whether glutamate regulates the dynamin-independent endocytosis in astrocytes. Astrocytes were first exposed to glutamate to induce intracellular Ca^{2+} oscillation and then stained with FM1-43. The FM signal was remarkably enhanced in glutamate-treated cells compared with the control group (Fig. 9*A*,*B*,*D*) ($n = 19–20$; $p < 0.001$). Pretreatment of astrocytes with MCPG mostly abolished the effect of glutamate on the dynamin-independent endocytosis (Fig. 9*C*,*D*). These results further indicate that the dynamin-independent endocytosis in astrocytes is tightly coupled to the intracellular Ca^{2+} signaling. Since both ATP and glutamate can be released by neurons and astrocytes, their potent regulation on the dynamin-independent endocytosis in astrocytes suggests a potential novel interaction between neurons and glial cells.

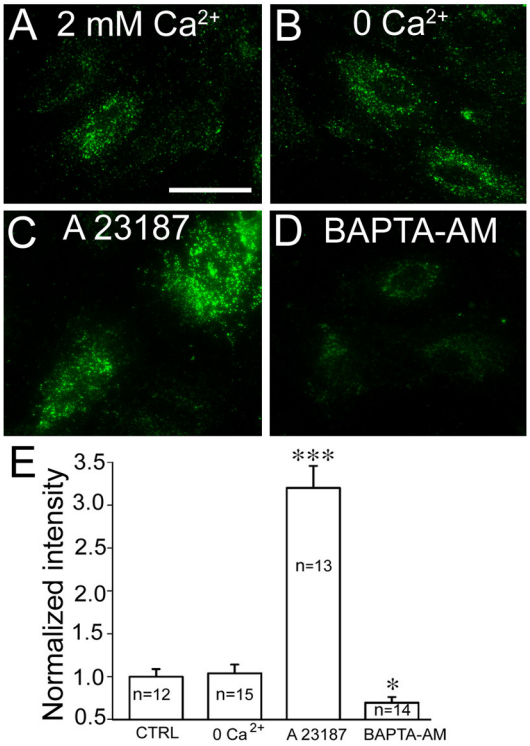

Figure 7. Dynamin-independent endocytosis in astrocytes is regulated by intracellular but not extracellular Ca^{2+}. ***A***, ***B***, Fluorescence images of astrocytes stained with 20 μM FM1-43 for 3 min in normal bath solution with 2 mM Ca^{2+} (***A***) or in Ca^{2+}-free bath solution (***B***). Scale bar, 50 μm. ***C***, FM image of astrocytes pretreated with Ca^{2+} ionophore A23187 (10 μM; 10 min) to increase intracellular Ca^{2+}. ***D***, FM image of astrocytes pretreated with Ca^{2+} chelator BAPTA-AM (25 μM; 45 min) to decrease intracellular Ca^{2+}. FM signal was enhanced by A23187, but decreased after BAPTA-AM treatment. ***E***, Normalized intensity of FM signal after different treatments relative to the control group (0 Ca^{2+}, 104 ± 10% of control, $n = 15$, $p > 0.7$; A23187, 320 ± 30% of control, $n = 13$, ***$p < 0.001$; BAPTA-AM, 70 ± 6% of control, $n = 14$, *$p < 0.02$). Error bars indicate SEM.

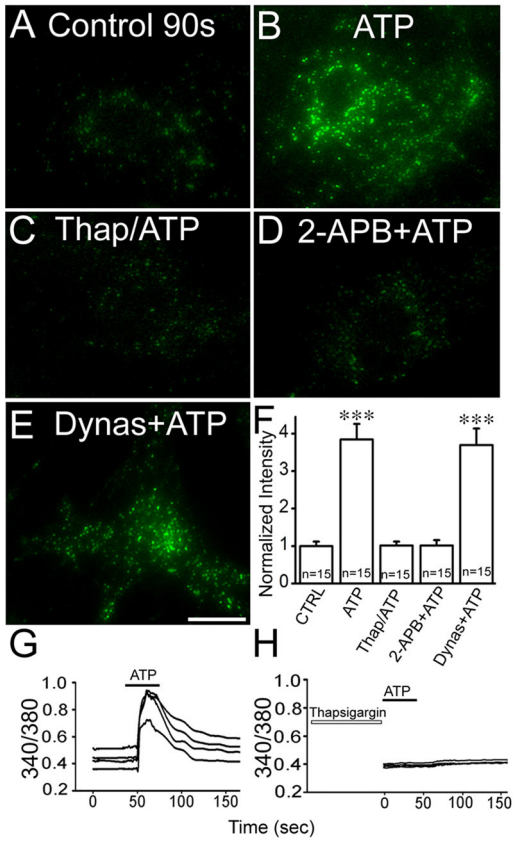

Figure 8. ATP regulates dynamin-independent endocytosis in astrocytes through intracellular Ca^{2+} signaling. ***A***, ***B***, Images of astrocytes stained with FM1-43 (20 μM) for 90 s in Ca^{2+}-free bath solution without (***A***) or with ATP (10 μM) (***B***). Note a substantial enhancement of FM signal in the presence of ATP. ***C***, FM image of astrocytes pretreated with thapsigargin (10 μM; 10 min) to deplete internal Ca^{2+} store and then loaded with FM1-43 (90 s) in the presence of ATP. No enhancement of the FM uptake was detected. ***D***, FM image of astrocytes pretreated with 2-APB (50 μM; 5 min) to block IP3 receptors and then loaded with FM1-43 in the presence of ATP. ***E***, FM image of astrocytes pretreated with dynasore (50 μM; 30 min) to block dynamin activity and then loaded with FM1-43 in the presence of ATP. Scale bar, 50 μm. ***F***, Normalized intensity of FM signal after different drug treatments. FM intensity was significantly increased after ATP treatment (384 ± 40% of control; $n = 15$; ***$p < 0.001$), but such enhancement was abolished by pretreatment with thapsigargin (101 ± 14%; $n = 15$; $p > 0.9$) or with 2-APB (101 ± 10%; $n = 15$; $p > 0.9$). The enhancement of ATP was not affected by dynasore treatment (370 ± 44% of control; $n = 15$; $p < 0.001$). Error bars indicate SEM. ***G***, Ca^{2+} imaging recordings showing that acute application of ATP (10 μM) induced a significant increase of intracellular Ca^{2+} in astrocytes. ***H***, Ca^{2+} imaging showing that pretreatment with thapsigargin (10 μM; 10 min) blocked the increase of intracellular Ca^{2+} induced by ATP.

Amyloid-β peptide regulates astroglial rapid endocytosis

Malfunction of astrocytes have been implied in Alzheimer's disease characterized by an accumulation of Aβ peptides in senile plaques (Nagele et al., 2004). Among different Aβ variants, Aβ1–42 is a key element in Aβ plaques (Zameer et al., 2006). Recent studies showed that both the full-length peptide Aβ1–42 and its essential neurotoxic fragment Aβ25–35 can induce robust intracellular Ca^{2+} transients in cultured astrocytes (Abramov et al., 2003). We therefore hypothesized that Aβ might regulate the dynamin-independent endocytosis in astrocytes. To test this idea, we first examined whether Aβ triggers intracellular Ca^{2+} transients in our cultured astrocytes. Indeed, Ca^{2+} imaging showed robust Ca^{2+} transients when astrocytes were exposed to Aβ1–42 (Fig. 9*K*). No Ca^{2+} transients were detected when cells were treated with the reverse peptide Aβ42–1 (data not shown). Next, we examined the effect of Aβ on the dynamin-independent endocytosis in astrocytes. Cells were pretreated with Aβ1–42 for 15 min and then stained with FM1-43 for 3 min. For control experiments, cells were treated with reverse Aβ peptide or without any treatment. No difference was found in the FM dye uptake between astrocytes treated with reverse Aβ or simply with normal bath solution (Fig. 9*G*,*H*,*J*). In contrast, treatment with Aβ1–42 peptide significantly enhanced the FM dye uptake in astrocytes (Fig. 9*I*,*J*) ($n = 13$; $p < 0.01$). In addition, we also examined the active short fragment Aβ25–35 and found a similar enhancement on the dynamin-independent endocytosis (supplemental Fig. 6, available at www.jneurosci.org as supplemental material). These data indicate that the novel endocytic pathway revealed by live FM imaging in astrocytes can be regulated not only by physiological stimulants but also by pathological agents such as Aβ peptides.

Discussion

Compared with clathrin- or caveolin-dependent endocytosis, the function and regulation of clathrin- and caveolin-independent endocytic pathways are poorly understood. Here, we demonstrate that a constitutive endocytosis in astrocytes is independent of clathrin and caveolin. This constitutive endocytic pathway in astrocytes has several key features, which have been summarized into a working model (Fig. 10). First, the dynamin-independent endocytosis is independent of dynamin but regulated by Rab5. Second, the vesicles after dynamin-independent endocytosis are

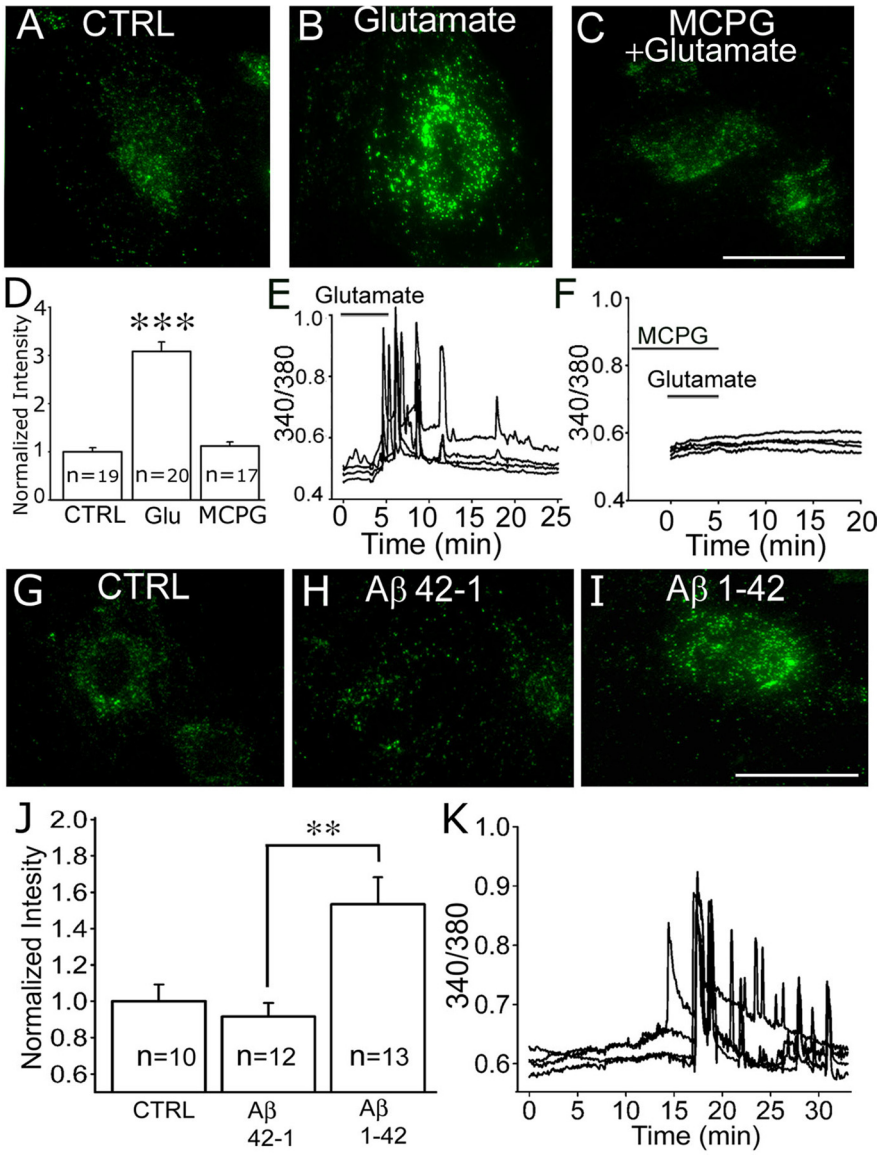

Figure 9. Dynamin-independent endocytosis in astrocytes is enhanced by glutamate and amyloid-β peptide. ***A***, ***B***, FM images of astrocytes in control (***A***) or pretreated with glutamate (1 mM; 5 min) (***B***). Glutamate significantly enhanced the uptake of FM dye. ***C***, FM image of astrocytes pretreated with mGluR antagonist MCPG (200 μM) before and during glutamate stimulation. ***D***, Normalized intensity of FM signal under control, glutamate, and glutamate plus MCPG conditions. Glutamate significantly increased the FM intensity (310 $\pm$ 20% of control; $n = 20$; ***$p < 0.001$), but the enhancement was blocked by pretreatment with MCPG (110 $\pm$ 10%; $n = 17$; $p > 0.3$). Error bars indicate SEM. ***E***, Ca^{2+} imaging traces showing transient increase of intracellular Ca^{2+} in astrocytes induced by glutamate application (1 mM). ***F***, Pretreatment with MCPG (200 μM) blocked the Ca^{2+} increase induced by glutamate application. ***G–I***, FM images of astrocytes under control (***G***), pretreatment with reverse peptide Aβ42–1 (50 μM; 20 min) (***H***), or active peptide Aβ1–42 (50 μM; 20 min) (***I***). ***J***, Normalized intensity of FM signal under different treatments. FM intensity significantly increased in Aβ1–42 treatment group (150 $\pm$ 10% of control; $n = 12$; **$p < 0.002$) compared with the mock treatment with Aβ42–1 (92 $\pm$ 8% of control; $n = 13$). ***K***, Ca^{2+} imaging traces showing intracellular Ca^{2+} increase in astrocytes induced by application of Aβ1–42 (50 μM). Scale bars: ***A–C***, ***G–I***, 50 μm.

highly mobile and are quickly targeted to late endosomes/lysosomes in a few minutes. Third, the dynamin-independent endocytosis in astrocytes is tightly regulated by ATP and glutamate through elevating the intracellular Ca^{2+} concentration. Finally, Aβ peptides also significantly regulate the dynamin-independent endocytosis by triggering Ca^{2+} oscillation in astrocytes. This dynamin-independent endocytosis can uptake ATP analog and Aβ peptides, suggesting an important function in both physiological and pathological conditions.

Clathrin- and dynamin-independent endocytic pathway in astrocytes

The clathrin/dynamin independence and Ca^{2+} dependence of the astroglial endocytosis identified here represent a unique endocytic pathway (Lamaze et al., 2001; Sabharanjak et al., 2002). The dynamin-independent endocytic pathway in astrocytes is not targeted to Golgi complex (supplemental Fig. 4, available at www.jneurosci.org as supplemental material). This finding implies that signaling molecules internalized through the dynamin-independent endocytosis may not be mixed with those entering through clathrin- or caveolin-mediated pathway. Such distinct endocytic routes may be critical to ensure signaling specificity.

Dynamin-independent pathways have been reported in different cell types (Zhang et al., 2004a; Bonazzi et al., 2005; Xu et al., 2008). In dorsal root ganglion neurons, a dynamin-independent form of endocytosis was reported that is also independent of Ca^{2+} but can be induced by membrane depolarization (Zhang et al., 2004a). In nerve terminals of the calyx of Held, synaptic vesicles normally undergo dynamin-dependent endocytosis, but under intense stimulation, a form of dynamin-independent endocytosis can be activated (Xu et al., 2008). Although dynamin-independent endocytosis exists in nerve terminals, it is likely the dynamin-dependent endocytosis assuming the major functional role to maintain normal synaptic activity (Newton et al., 2006; Ferguson et al., 2007). In contrast, here we identify the dynamin-independent endocytosis as the major pathway in astrocytes under resting conditions. Such dynamin-independent endocytosis in astrocytes may have an important function in the uptake of nutrients. Dynamin-independent endocytosis may be regulated by other small GTPases such as Cdc42 or Arf1/Arf6 (Sabharanjak et al., 2002; Naslavsky et al., 2004; Mayor and Pagano, 2007; Kumari and Mayor, 2008), and the scission function may be mediated by flotillin or BARS (brefeldin A-ribosylated substrate) (Bonazzi et al., 2005; Glebov et al., 2006). Additional work is necessary to identify the molecular identity underlying the dynamin-independent endocytosis in astrocytes.

Caveolar endocytosis may represent a special type of lipid raft-mediated membrane endocytosis. Is it possible that the rapid endocytosis we identified in astrocytes is not dependent on caveolae but still dependent on lipid raft? Since lipid rafts are highly enriched with sphingolipids and cholesterol, a fluorescent sphingolipid analog such as BODIPY-LacCer (*N*-[5-(5,7-dimethyl boron dipyrromethene diXuoride)-1-pentanoyl]-1′,1-lactosyl-D-erythro-sphingosine) has been used to label lipid rafts

and study membrane trafficking (Marks et al., 2005; Singh et al., 2007). Filipin is widely used to disrupt lipid raft-mediated endocytosis because it binds cholesterol and makes membrane rigid (Naslavsky et al., 2004; Sigismund et al., 2008). Therefore, we used lipid raft marker BODIPY-LacCer and filipin to investigate the relationship between lipid raft and the FM-labeled rapid endocytic pathway in astrocytes. We found that the uptake of BODIPY-LacCer is a relatively slow process compared with the rapid endocytosis of FM dye (supplemental Fig. 7*A*,*B*, available at www.jneurosci.org as supplemental material). Unlike FM dye uptake, the endocytosis of BODIPY-LacCer was dependent on dynamin because of the inhibition by dynasore (supplemental Fig. 7*C*,*D*, available at www.jneurosci.org as supplemental material), consistent with previous findings in fibroblasts (Puri et al., 2001). We further tested the effect of filipin on the endocytosis of FM dye and BODIPY-LacCer in astrocytes under two conditions: a milder one at 1 μg/ml for 20 min (supplemental Fig. 8, available at www.jneurosci.org as supplemental material) and a stronger one at 2 μg/ml for 1 h (supplemental Fig. 9, available at www.jneurosci.org as supplemental material). Whereas both filipin treatment significantly inhibited BODIPY-LacCer endocytosis, only stronger filipin treatment had a significant effect on the endocytosis of FM dye. In summary, the rapid endocytosis in astrocytes appears to be different from lipid raft-mediated endocytosis. However, strong perturbation of membrane cholesterol by filipin can affect the rapid endocytosis, possibly because of a disruption of membrane signaling system or abnormal membrane rigidity that impairs membrane invaginations. In fact, dynamin-independent but filipin-sensitive endocytic pathway has been reported in the literature (Vidricaire and Tremblay, 2007). Additionally, filipin is membrane permeable and might have complicated effects on internal membrane organelles as well.

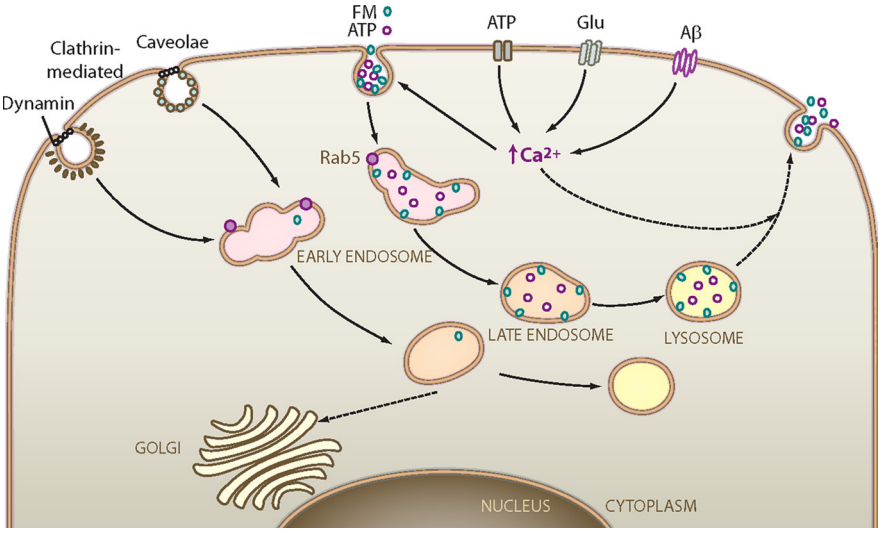

Figure 10. A working model illustrating the Ca^{2+}-regulated dynamin-independent endocytic pathway in astrocytes. The clathrin- and caveolin-dependent endocytic pathways are shown on the left. They are also dynamin dependent. The clathrin/dynamin-independent endocytic pathway is shown on the right, which is regulated by Rab5 and intracellular Ca^{2+}. ATP, glutamate, and Aβ peptides all regulate the dynamin-independent endocytosis through elevating intracellular Ca^{2+} in astrocytes.

After rapid endocytosis, vesicles move along microtubules to transport internalized molecules into late endosomes/lysosomes for degradation or for storage. Recent studies suggest that ATP may be stored inside lysosomes and then released through lysosomal fusion with plasma membranes (Jaiswal et al., 2007; Zhang et al., 2007; Li et al., 2008). The overall process of lysosomal exocytosis appears to be slower than the dynamin-independent endocytosis reported here. The dynamin-independent endocytosis in astrocytes has to be counterbalanced by a rapid exocytosis to maintain membrane surface stability. The nature of a potential constitutive exocytosis in astrocytes is yet to be identified in future studies.

Ca^{2+} regulation of astroglial endocytosis

Astrocytes respond to a variety of stimuli including mechanical, electrical, and chemical stimulation with a substantial change in the intracellular Ca^{2+} signaling. We found that the dynamin-independent endocytosis in astrocytes is tightly regulated by ATP and glutamate through intracellular Ca^{2+}, suggesting a close relationship between endocytosis and environmental changes. At resting state, the dynamin-independent endocytosis in astrocytes is constitutive but kept at a low level, possibly because of very low concentration of resting intracellular Ca^{2+}. Decrease or increase intracellular Ca^{2+} in astrocytes will downregulate or upregulate the dynamin-independent endocytosis correspondingly (Fig. 7). Such strong Ca^{2+}-dependent endocytosis is not common among mammalian cells except synaptic vesicle endocytosis in nerve terminals (Chen et al., 2003; Wu et al., 2005). However, synaptic vesicle cycling at nerve terminals is mostly dependent on extracellular Ca^{2+}, whereas the dynamin-independent endocytosis in astrocytes is not affected by extracellular Ca^{2+} but depends solely on intracellular Ca^{2+}. Another difference is that synaptic vesicle endocytosis is clathrin mediated, whereas the dynamin-independent endocytosis in astrocytes is not. The major regulatory factor in controlling the dynamin-independent endocytosis in astrocytes appears to be the Ca^{2+} release from internal Ca^{2+} stores, regardless of what kind of stimulation that triggers the Ca^{2+} increase. Since Ca^{2+} wave propagates among neighboring astrocytes, it is possible that astrocytes may simultaneously increase the dynamin-independent endocytosis to buffer small molecules in a local environment (Parri et al., 2001; Fellin et al., 2006; Wang et al., 2006).

Function of the dynamin-independent endocytosis in astrocytes

One important function of astroglial cells in the brain is to uptake nutrients from blood vessels (Prat et al., 2001). Although clathrin-mediated endocytosis is responsible for the internalization of membrane receptors, many soluble nutrients may be internalized by astrocytes through the dynamin-independent endocytosis characterized here. In resting conditions, the rapid and constitutive endocytosis in astrocytes can provide steady nutrient supply for glial cells as well as neurons. Unlike clathrin- or caveolin-dependent endocytosis, which selectively internalizes specific proteins or lipids, the dynamin-independent endocytosis is likely nondiscriminative in internalizing soluble molecules. However, after endocytosis, internalized molecules will be sorted through Rab5-dependent early endosomes, in which nutrient molecules may be separated from other soluble molecules. After endosomal sorting, many soluble molecules will be transported to lysosomes for degradation or storage.

In addition to nutrient uptake, another important function of

the dynamin-independent endocytosis in astrocytes may be to regulate cell signaling in response to environmental stimulation. We demonstrate that both ATP and glutamate stimulation can significantly enhance the dynamin-independent endocytosis in astrocytes. ATP and glutamate can be released by both neurons and astrocytes to modulate astroglial and neuronal functions. Therefore, the regulation of the dynamin-independent endocytosis in astrocytes may represent a novel converging point during neuron–glial interactions. In addition to physiological functions, ATP release is often associated with pathological conditions, such as stress, hypoxia, and inflammation (Bodin and Burnstock, 2001). Therefore, ATP-induced transient increase of the dynamin-independent endocytosis in astrocytes can potentially serve as a neural protective mechanism by quickly internalizing cytotoxic molecules for degradation.

Pathological implication of the Aβ regulation of astroglial endocytosis

Malfunction of astrocytes are involved in many neurological disorders including Alzheimer's disease, ischemia, and stroke (Schubert et al., 2001; Takuma et al., 2004). Alzheimer's disease is characterized by substantial deposits of Aβ peptides forming plaques in the brain (Goedert and Spillantini, 2006; Haass and Selkoe, 2007). Aβ may be cytotoxic to neurons as well as astrocytes. Consistent with previous work (Abramov et al., 2003), our studies found that Aβ peptides evoke intracellular Ca^{2+} oscillations in cultured astrocytes. More importantly, Aβ significantly enhances the dynamin-independent endocytosis in astrocytes, which in turn can uptake or remove Aβ peptides (Fig. 9; supplemental Fig. 5, available at www.jneurosci.org as supplemental material). Unlike the transient release of ATP and glutamate through vesicular exocytosis (Montana et al., 2006), Aβ peptides can gradually accumulate in aging brains, which might have detrimental effects on glial endocytosis in addition to many other reported actions. Considering the fundamental roles of astrocytes in regulating brain functions, we postulate that abnormal regulation of the dynamin-independent endocytosis in astrocytes may contribute to neurological disorders such as Alzheimer's disease.

References

Abramov AY, Canevari L, Duchen MR (2003) Changes in intracellular calcium and glutathione in astrocytes as the primary mechanism of amyloid neurotoxicity. J Neurosci 23:5088–5095.

Araque A, Li N, Doyle RT, Haydon PG (2000) SNARE protein-dependent glutamate release from astrocytes. J Neurosci 20:666–673.

Benmerah A, Lamaze C (2007) Clathrin-coated pits: vive la difference? Traffic 8:970–982.

Betz WJ, Bewick GS (1992) Optical analysis of synaptic vesicle recycling at the frog neuromuscular junction. Science 255:200–203.

Bezzi P, Gundersen V, Galbete JL, Seifert G, Steinhäuser C, Pilati E, Volterra A (2004) Astrocytes contain a vesicular compartment that is competent for regulated exocytosis of glutamate. Nat Neurosci 7:613–620.

Bodin P, Burnstock G (2001) Purinergic signalling: ATP release. Neurochem Res 26:959–969.

Bonazzi M, Spanò S, Turacchio G, Cericola C, Valente C, Colanzi A, Kweon HS, Hsu VW, Polishchuck EV, Polishchuck RS, Sallese M, Pulvirenti T, Corda D, Luini A (2005) CtBP3/BARS drives membrane fission in dynamin-independent transport pathways. Nat Cell Biol 7:570–580.

Cameron PL, Liu C, Smart DK, Hantus ST, Fick JR, Cameron RS (2002) Caveolin-1 expression is maintained in rat and human astroglioma cell lines. Glia 37:275–290.

Chen J, Backus KH, Deitmer JW (1997) Intracellular calcium transients and potassium current oscillations evoked by glutamate in cultured rat astrocytes. J Neurosci 17:7278–7287.

Chen X, Wang L, Zhou Y, Zheng LH, Zhou Z (2005) "Kiss-and-run" glutamate secretion in cultured and freshly isolated rat hippocampal astrocytes. J Neurosci 25:9236–9243.

Chen Y, Deng L, Maeno-Hikichi Y, Lai M, Chang S, Chen G, Zhang JF (2003) Formation of an endophilin-Ca^{2+} channel complex is critical for clathrin-mediated synaptic vesicle endocytosis. Cell 115:37–48.

Cheng ZJ, Singh RD, Marks DL, Pagano RE (2006) Membrane microdomains, caveolae, and caveolar endocytosis of sphingolipids. Mol Membr Biol 23:101–110.

Conner SD, Schmid SL (2003) Regulated portals of entry into the cell. Nature 422:37–44.

Damke H, Baba T, Warnock DE, Schmid SL (1994) Induction of mutant dynamin specifically blocks endocytic coated vesicle formation. J Cell Biol 127:915–934.

Dessy C, Kelly RA, Balligand JL, Feron O (2000) Dynamin mediates caveolar sequestration of muscarinic cholinergic receptors and alteration in NO signaling. EMBO J 19:4272–4280.

Fellin T, Sul JY, D'Ascenzo M, Takano H, Pascual O, Haydon PG (2006) Bidirectional astrocyte-neuron communication: the many roles of glutamate and ATP. Novartis Found Symp 276:208–217; discussion 217–221, 233–237, 275–281.

Ferguson SM, Brasnjo G, Hayashi M, Wölfel M, Collesi C, Giovedi S, Raimondi A, Gong LW, Ariel P, Paradise S, O'toole E, Flavell R, Cremona O, Miesenböck G, Ryan TA, De Camilli P (2007) A selective activity-dependent requirement for dynamin 1 in synaptic vesicle endocytosis. Science 316:570–574.

Fiacco TA, McCarthy KD (2006) Astrocyte calcium elevations: properties, propagation, and effects on brain signaling. Glia 54:676–690.

Glebov OO, Bright NA, Nichols BJ (2006) Flotillin-1 defines a clathrin-independent endocytic pathway in mammalian cells. Nat Cell Biol 8:46–54.

Goedert M, Spillantini MG (2006) A century of Alzheimer's disease. Science 314:777–781.

Gruenberg J (2001) The endocytic pathway: a mosaic of domains. Nat Rev Mol Cell Biol 2:721–730.

Guthrie PB, Knappenberger J, Segal M, Bennett MV, Charles AC, Kater SB (1999) ATP released from astrocytes mediates glial calcium waves. J Neurosci 19:520–528.

Haass C, Selkoe DJ (2007) Soluble protein oligomers in neurodegeneration: lessons from the Alzheimer's amyloid beta-peptide. Nat Rev Mol Cell Biol 8:101–112.

He Z, Fan J, Kang L, Lu J, Xue Y, Xu P, Xu T, Chen L (2008) Ca^{2+} triggers a novel clathrin-independent but actin-dependent fast endocytosis in pancreatic beta cells. Traffic 9:910–923.

Herskovits JS, Burgess CC, Obar RA, Vallee RB (1993) Effects of mutant rat dynamin on endocytosis. J Cell Biol 122:565–578.

Jaiswal JK, Fix M, Takano T, Nedergaard M, Simon SM (2007) Resolving vesicle fusion from lysis to monitor calcium-triggered lysosomal exocytosis in astrocytes. Proc Natl Acad Sci U S A 104:14151–14156.

Jiang M, Chen G (2006) High Ca^{2+}-phosphate transfection efficiency in low-density neuronal cultures. Nat Protoc 1:695–700.

Jourdain P, Bergersen LH, Bhaukaurally K, Bezzi P, Santello M, Domercq M, Matute C, Tonello F, Gundersen V, Volterra A (2007) Glutamate exocytosis from astrocytes controls synaptic strength. Nat Neurosci 10:331–339.

Kay AR, Alfonso A, Alford S, Cline HT, Holgado AM, Sakmann B, Snitsarev VA, Stricker TP, Takahashi M, Wu LG (1999) Imaging synaptic activity in intact brain and slices with FM1-43 in *C. elegans*, lamprey, and rat. Neuron 24:809–817.

Kirkham M, Fujita A, Chadda R, Nixon SJ, Kurzchalia TV, Sharma DK, Pagano RE, Hancock JF, Mayor S, Parton RG (2005) Ultrastructural identification of uncoated caveolin-independent early endocytic vehicles. J Cell Biol 168:465–476.

Kreft M, Stenovec M, Rupnik M, Grilc S, Krzan M, Potokar M, Pangrsic T, Haydon PG, Zorec R (2004) Properties of Ca^{2+}-dependent exocytosis in cultured astrocytes. Glia 46:437–445.

Krzan M, Stenovec M, Kreft M, Pangrsic T, Grilc S, Haydon PG, Zorec R (2003) Calcium-dependent exocytosis of atrial natriuretic peptide from astrocytes. J Neurosci 23:1580–1583.

Kumari S, Mayor S (2008) ARF1 is directly involved in dynamin-independent endocytosis. Nat Cell Biol 10:30–41.

Lamaze C, Schmid SL (1995) The emergence of clathrin-independent pinocytic pathways. Curr Opin Cell Biol 7:573–580.

Lamaze C, Dujeancourt A, Baba T, Lo CG, Benmerah A, Dautry-Varsat A (2001) Interleukin 2 receptors and detergent-resistant membrane domains define a clathrin-independent endocytic pathway. Mol Cell 7:661–671.

Li D, Ropert N, Koulakoff A, Giaume C, Oheim M (2008) Lysosomes are the major vesicular compartment undergoing Ca^{2+}-regulated exocytosis from cortical astrocytes. J Neurosci 28:7648–7658.

Macia E, Ehrlich M, Massol R, Boucrot E, Brunner C, Kirchhausen T (2006) Dynasore, a cell-permeable inhibitor of dynamin. Dev Cell 10:839–850.

Marks DL, Singh RD, Choudhury A, Wheatley CL, Pagano RE (2005) Use of fluorescent sphingolipid analogs to study lipid transport along the endocytic pathway. Methods 36:186–195.

Maxfield FR, McGraw TE (2004) Endocytic recycling. Nat Rev Mol Cell Biol 5:121–132.

Mayor S, Pagano RE (2007) Pathways of clathrin-independent endocytosis. Nat Rev Mol Cell Biol 8:603–612.

McCarthy KD, de Vellis J (1980) Preparation of separate astroglial and oligodendroglial cell cultures from rat cerebral tissue. J Cell Biol 85:890–902.

Montana V, Malarkey EB, Verderio C, Matteoli M, Parpura V (2006) Vesicular transmitter release from astrocytes. Glia 54:700–715.

Mousavi SA, Malerød L, Berg T, Kjeken R (2004) Clathrin-dependent endocytosis. Biochem J 377:1–16.

Nagele RG, Wegiel J, Venkataraman V, Imaki H, Wang KC, Wegiel J (2004) Contribution of glial cells to the development of amyloid plaques in Alzheimer's disease. Neurobiol Aging 25:663–674.

Naslavsky N, Weigert R, Donaldson JG (2004) Characterization of a nonclathrin endocytic pathway: membrane cargo and lipid requirements. Mol Biol Cell 15:3542–3552.

Newton AJ, Kirchhausen T, Murthy VN (2006) Inhibition of dynamin completely blocks compensatory synaptic vesicle endocytosis. Proc Natl Acad Sci U S A 103:17955–17960.

Parpura V, Basarsky TA, Liu F, Jeftinija K, Jeftinija S, Haydon PG (1994) Glutamate-mediated astrocyte-neuron signalling. Nature 369:744–747.

Parri HR, Gould TM, Crunelli V (2001) Spontaneous astrocytic Ca^{2+} oscillations in situ drive NMDAR-mediated neuronal excitation. Nat Neurosci 4:803–812.

Parton RG, Simons K (2007) The multiple faces of caveolae. Nat Rev Mol Cell Biol 8:185–194.

Pelkmans L, Helenius A (2002) Endocytosis via caveolae. Traffic 3:311–320.

Prat A, Biernacki K, Wosik K, Antel JP (2001) Glial cell influence on the human blood-brain barrier. Glia 36:145–155.

Puri V, Watanabe R, Singh RD, Dominguez M, Brown JC, Wheatley CL, Marks DL, Pagano RE (2001) Clathrin-dependent and -independent internalization of plasma membrane sphingolipids initiates two Golgi targeting pathways. J Cell Biol 154:535–547.

Qian ZM, To Y, Tang PL, Feng YM (1999) Transferrin receptors on the plasma membrane of cultured rat astrocytes. Exp Brain Res 129:473–476.

Rink J, Ghigo E, Kalaidzidis Y, Zerial M (2005) Rab conversion as a mechanism of progression from early to late endosomes. Cell 122:735–749.

Roberts RL, Barbieri MA, Pryse KM, Chua M, Morisaki JH, Stahl PD (1999) Endosome fusion in living cells overexpressing GFP-rab5. J Cell Sci 112:3667–3675.

Sabharanjak S, Sharma P, Parton RG, Mayor S (2002) GPI-anchored proteins are delivered to recycling endosomes via a distinct cdc42-regulated, clathrin-independent pinocytic pathway. Dev Cell 2:411–423.

Salter MW, Hicks JL (1994) ATP-evoked increases in intracellular calcium in neurons and glia from the dorsal spinal cord. J Neurosci 14:1563–1575.

Schools GP, Kimelberg HK (2001) Metabotropic glutamate receptors in freshly isolated astrocytes from rat hippocampus. Prog Brain Res 132:301–312.

Schubert P, Ogata T, Marchini C, Ferroni S (2001) Glia-related pathomechanisms in Alzheimer's disease: a therapeutic target? Mech Ageing Dev 123:47–57.

Sever S (2002) Dynamin and endocytosis. Curr Opin Cell Biol 14:463–467.

Sigismund S, Argenzio E, Tosoni D, Cavallaro E, Polo S, Di Fiore PP (2008) Clathrin-mediated internalization is essential for sustained EGFR signaling but dispensable for degradation. Dev Cell 15:209–219.

Singh RD, Marks DL, Pagano RE (2007) Using fluorescent sphingolipid analogs to study intracellular lipid trafficking. Curr Protoc Cell Biol 24:24.1.

Sorkin A, Von Zastrow M (2002) Signal transduction and endocytosis: close encounters of many kinds. Nat Rev Mol Cell Biol 3:600–614.

Stenmark H, Parton RG, Steele-Mortimer O, Lütcke A, Gruenberg J, Zerial M (1994) Inhibition of rab5 GTPase activity stimulates membrane fusion in endocytosis. EMBO J 13:1287–1296.

Suadicani SO, Brosnan CF, Scemes E (2006) P2X7 receptors mediate ATP release and amplification of astrocytic intercellular Ca^{2+} signaling. J Neurosci 26:1378–1385.

Takuma K, Baba A, Matsuda T (2004) Astrocyte apoptosis: implications for neuroprotection. Prog Neurobiol 72:111–127.

Thomsen P, Roepstorff K, Stahlhut M, van Deurs B (2002) Caveolae are highly immobile plasma membrane microdomains, which are not involved in constitutive endocytic trafficking. Mol Biol Cell 13:238–250.

Vidricaire G, Tremblay MJ (2007) A clathrin, caveolae, and dynamin-independent endocytic pathway requiring free membrane cholesterol drives HIV-1 internalization and infection in polarized trophoblastic cells. J Mol Biol 368:1267–1283.

Volterra A, Meldolesi J (2005) Astrocytes, from brain glue to communication elements: the revolution continues. Nat Rev Neurosci 6:626–640.

Wang X, Lou N, Xu Q, Tian GF, Peng WG, Han X, Kang J, Takano T, Nedergaard M (2006) Astrocytic Ca^{2+} signaling evoked by sensory stimulation in vivo. Nat Neurosci 9:816–823.

Wu W, Xu J, Wu XS, Wu LG (2005) Activity-dependent acceleration of endocytosis at a central synapse. J Neurosci 25:11676–11683.

Xu J, McNeil B, Wu W, Nees D, Bai L, Wu LG (2008) GTP-independent rapid and slow endocytosis at a central synapse. Nat Neurosci 11:45–53.

Yao J, Qi J, Chen G (2006) Actin-dependent activation of presynaptic silent synapses contributes to long-term synaptic plasticity in developing hippocampal neurons. J Neurosci 26:8137–8147.

Zameer A, Schulz P, Wang MS, Sierks MR (2006) Single chain Fv antibodies against the 25–35 Abeta fragment inhibit aggregation and toxicity of Abeta42. Biochemistry 45:11532–11539.

Zerial M, McBride H (2001) Rab proteins as membrane organizers. Nat Rev Mol Cell Biol 2:107–117.

Zhang C, Xiong W, Zheng H, Wang L, Lu B, Zhou Z (2004a) Calcium- and dynamin-independent endocytosis in dorsal root ganglion neurons. Neuron 42:225–236.

Zhang Q, Pangrsic T, Kreft M, Krzan M, Li N, Sul JY, Halassa M, Van Bockstaele E, Zorec R, Haydon PG (2004b) Fusion-related release of glutamate from astrocytes. J Biol Chem 279:12724–12733.

Zhang Z, Chen G, Zhou W, Song A, Xu T, Luo Q, Wang W, Gu XS, Duan S (2007) Regulated ATP release from astrocytes through lysosome exocytosis. Nat Cell Biol 9:945–953.